Published online 6 February 2007

Nucleic Acids Research, 2007, Vol. 35, No. 5 ***1421–1431***
doi:10.1093/nar/gkl1164

Deinococcus glutaminyl-tRNA synthetase is a chimer between proteins from an ancient and the modern pathways of aminoacyl-tRNA formation

Marzanna Deniziak, Claude Sauter, Hubert Dominique Becker*, Caroline Alexandra Paulus, Richard Giegé and Daniel Kern

UPR 9002 'Architecture et Reactivité de l'ARN', Université Louis Pasteur, Institut de Biologie Moléculaire et Cellulaire du CNRS, 15, Rue René Descartes, F-67084 Strasbourg Cedex, France

Received December 20, 2006; Accepted December 20, 2006

ABSTRACT

Glutaminyl-tRNA synthetase from *Deinococcus radiodurans* possesses a C-terminal extension of 215 residues appending the anticodon-binding domain. This domain constitutes a paralog of the Yqey protein present in various organisms and part of it is present in the C-terminal end of the GatB subunit of GatCAB, a partner of the indirect pathway of Gln-tRNA^{Gln} formation. To analyze the peculiarities of the structure–function relationship of this GlnRS related to the Yqey domain, a structure of the protein was solved from crystals diffracting at 2.3 Å and a docking model of the synthetase complexed to tRNA^{Gln} constructed. The comparison of the modeled complex with the structure of the *E. coli* complex reveals that all residues of *E. coli* GlnRS contacting tRNA^{Gln} are conserved in *D. radiodurans* GlnRS, leaving the functional role of the Yqey domain puzzling. Kinetic investigations and tRNA-binding experiments of full length and Yqey-truncated GlnRSs reveal that the Yqey domain is involved in tRNA^{Gln} recognition. They demonstrate that Yqey plays the role of an affinity-enhancer of GlnRS for tRNA^{Gln} acting only in *cis*. However, the presence of Yqey in free state in organisms lacking GlnRS, suggests that this domain may exert additional cellular functions.

INTRODUCTION

Flawless protein translation requires a full set of 20 types of perfectly paired aminoacyl-tRNAs. It was *de facto* expected that each cell should possess a full set of 20 aminoacyl-tRNA synthetases capable of matching each of the 20 natural amino acids to the cognate tRNAs (1). Recent studies on synthesis of glutaminyl-tRNA^{Gln} have forced a revision of this assumption (2). This aminoacylated tRNA displays the unique feature of being formed by kingdom-specific pathways (3,4). Eukaryotes and a small subset of bacteria use the common route of tRNA aminoacylation, whereby the GlnRSs attach glutamine directly onto tRNA^{Gln} (5). The majority of bacteria and all archaea use an indirect pathway involving a tRNA-dependent amidotransferase that compensates for the absence of GlnRS (3,4,6,7). In this alternate route, glutamyl-tRNA^{Gln}, a misacylated species formed by a non-discriminating GluRS (8), is amidated by a domain-specific AdT thereby generating the correctly paired glutaminyl-tRNA^{Gln} (3,4). In bacteria, AdTs are composed of three subunits, GatC, GatA and GatB assembled in a heterotrimeric enzyme called GatCAB (4,9,10). While half of the archaea possess this heterotrimeric AdT, they all possess an archaeal-specific AdT called GatDE (3,9–11). Transamidation-catalyzed formation of Gln-tRNA^{Gln} is so widespread among prokaryotes that GlnRS is rarely found in bacteria and has so far never been identified in archaea. *Deinococcus radiodurans* is one of those rare bacteria possessing a GlnRS (12,13).

All aaRSs are assembled piece-wise and often display domains appended to the two ubiquitous functional modules that are the catalytic and anticodon-binding domains (14–18). However, all bacterial GlnRSs studied so far lack any appended domain. The presence in *D. radiodurans* GlnRS of 220 additional amino acids drew our attention. This extension is located in the C-terminal part of the protein and constitutes an appendix of its anticodon-binding domain (12,19,20). Sequence comparison shows that the C-terminal half of this appendix is homologous to a family of bacterial and yeast proteins of unknown function named Yqey

*To whom correspondence should be addressed. Tel: +33 (0)3 88 41 70 41; Fax: +33 (0)3 88 60 22 18; Email: H.Becker@ibmc.u-strasbg.fr
Correspondence may also be addressed to Daniel Kern. Tel: +33 (0)3 88 41 70 92; Fax: +33 (0)3 88 60 22 18; Email: D.Kern@ibmc.u-strasbg.fr
The authors wish it to be known that, in their opinion, the first three authors should be regarded as joint First Authors.

(PFAM id: PF02637, 21). There are ~100 known Yqey proteins that on average are 150 amino-acid-long, and interestingly, share sequence homologies with the C-terminal domain of GatB and GatE, the tRNA-binding subunits of bacterial and archaeal AdTs (22,23). The presence of the *gatB* or *gatE* gene signals the presence of an AdT in an organism since the GatB and GatE subunits are exclusively found in association with the other subunits constituting the AdTs and, except the Yqey proteins, have no homologs. Among these proteins, the one encoded by *D. radiodurans* is unique (12). While in all organisms, when present, Yqey is encoded in an autonomous ORF, in *D. radiodurans* its gene is fused in frame downstream that of GlnRS. As a result, *Dr* GlnRS is formed by the fusion of structural protein modules involved in the direct and indirect pathways of glutaminyl-tRNA^{Gln} formation. In order to gain insight into the function of the Yqey domain appended to *Dr* GlnRS, functional and structural investigations were undertaken with this atypical aaRS. Remarkably, the Yqey domain has a disordered orientation in the structure of GlnRS where it acts as a tRNA^{Gln} affinity enhancer. Mechanistic implications are discussed.

MATERIALS AND METHODS

Materials

Hydroxyapatite CHT20 column was from Bio-Rad. L-[^{14}C]Gln (254 mCi·mmol^{-1}) was from Amersham, Dynazyme Taq polymerase from Finnzyme, restriction enzymes, chitin-agarose, pTYB11 vector and *E. coli* ER2566 strain were from New England Biolabs. *D. radiodurans* R1 strain was from DSMZ and was grown overnight at 37°C in glass flasks as described (24) and harvested at the end of the exponential phase ($A_{600\,nm} = 2.5$).

Cloning, expression and purification of native and truncated *D. radiodurans* GlnRSs

The ORFs of full length and C-terminal truncated *Dr* GlnRS (FL- and Δ-GlnRS) and of full length and N-terminal truncated Yqey domains (FL- and Δ-Yqey) were PCR-amplified using 100 ng genomic DNA and 100 pmol of each of the following primers: 5′-GGTGGG TGCTCTTCCAACATGGGGGCGTTTGGGTGGGA G-3′ (sense for FL- and Δ-GlnRS) and 5′-GGTG GTCTGCAGTCATTAGGCGAGAGCGTCTTTGAG CGC-3′ (anti-sense for FL-GlnRS) and 5′-GGTGGTCTG CAGTCATTAGCCGCCCTGCTTGCCCCAGG-3′ (anti-sense for Δ-GlnRS), 5′-GGTGGTTGCTCTTCCAA CATGACCCAGCAGAAGGCGGAAGGC-3′ (sense for FL-Yqey), 5′-GGTGGTTGTTCTTCCAACATGCGCA CCATCGCCCGTGAC CCG-3′ (sense for Δ-Yqey) and 5′-GGTGGTCGTCAGTCATTAGGCGACAGCGTCT TTG ACGC-3′ (anti-sense for FL- and Δ-Yqey). Reactions were run in the presence of 5% DMSO, and PCR products were hydrolyzed by *Sap*I and *Pst*I before ligation into pTYB11 expression vector upstream the sequence encoding the chitin-binding domain and the intein. Amplified sequences were controlled by sequencing, and proteins expressed in transformed *E. coli* ER2566 strain. Bacterial growth, induction by IPTG, cell disruption, crude extract preparation and FL-GlnRS purification were conducted as described (24). Δ-GlnRS, FL- and Δ-Yqey domains were purified on chitin-agarose and elution by self-cleavage of intein followed by chromatography on Bio-Scale CHT5-I ceramic hydroxyapatite. Purity was controlled by SDS-PAGE and mass spectrometry. Proteins were stored at −20°C in 50 mM Tris-HCl pH 8.0 containing 5 mM β-mercaptoethanol, 0.5 mM Na_2-EDTA and 50% glycerol. Molecular mass of *Dr* GlnRS was determined by mass spectrometry on a Bruker Biflex III apparatus.

Total tRNA and tRNA^{Gln} transcripts from *D. radiodurans*

Bacterial pellets (80 g) were treated with 95% ethanol to remove the cell outer membrane. After centrifugation, cells were suspended in 140 mM Na-acetate pH 4.5 containing 0.1% SDS. Nucleic acids were extracted with acid-buffered phenol and precipitated with ethanol. RNAs were recovered by centrifugation and total tRNA was obtained by isopropanol precipitation and chromatography on a DEAE-cellulose column (25). *Deinococcus radiodurans* tRNA$^{Gln(UUG)}$ and tRNA$^{Gln(CUG)}$ transcripts were obtained by *in vitro* transcription of the genes cloned under control of the T7 RNA polymerase promoter using the cassette cloning procedure (26). Since the two tRNAs start with 5′U known to prevent *in vitro* transcription, both genes were preceded by a sequence encoding a hammerhead ribozyme. Ribozyme-catalyzed self-cleavage and purification of transcripts were conducted as described (27).

Protein immunodetection

Sera containing antibodies directed against *Dr* FL-GlnRS (anti-FL-GlnRS) or *Thermus thermophilus* GatCAB AdT (anti-AdT) were obtained from immunized rabbits (28). Western- blots were performed with 0.05–1 μg of purified proteins electroblotted onto a nitrocellulose membrane (PROTRAN BA 83, pore size 0.2 μm, Schleicher and Schuell) after 10% (for FL-GlnRS and Δ-GlnRS) or 15% (for FL-Yqey and Δ-Yqey) SDS-PAGE. Membranes were incubated 1.5 h at room temperature in 50 μl of 20 mM Tris-HCl pH 7.5 containing 500 mM NaCl, 0.05% Tween and anti-FL-GlnRS or anti-AdT sera diluted 2000-fold. Antibodies bound to proteins were detected with peroxidase-conjugated anti-rabbit IgG in the presence of a bioluminescent reagent (ECL Kit, Amersham Bioscience). The ternary complexes were revealed by exposition of the membrane for 2–15 s on a X-ray film.

Gel-shift assays

Deinococcus radiodurans tRNA$^{Gln(UUG)}$ transcript was [^{32}P]-labeled at the 3′-end by exchange of its CCA trinucleotide. Five pmoles of transcript in 50-μl reaction mixture containing 50 mM Tris-HCl pH 8.0 and 10 mM $MgCl_2$ were treated with 10^{-3} unit of *Crotalus* venom phosphodiesterase for 10 min at 20°C. After phenol extraction and ethanol precipitation, the transcript without CCA, was incubated 30 min at 37°C in 50-μl reaction

mixture containing 1.8 μg of *E. coli* trinucleotidyl-tRNA transferase, 50 μCi α-[^{32}P]ATP, 50 μM CTP, 50 mM Tris-HCl pH 8.0, 10 mM $MgCl_2$ and 8 mM DTE. The radiolabeled tRNA was purified by 8 M urea PAGE (10%), electroeluted, precipitated with ethanol and renatured.

Complexes between GlnRS and Yqey and their variants and $tRNA^{Gln}$ were visualized by band-shift after PAGE fractionation and quantified. For that, constant amounts of $tRNA^{Gln}$ transcript (5×10^5 cpm) were incubated with increasing amounts of FL-GlnRS, △-GlnRS, FL-Yqey or △-Yqey in the presence of 10% glycerol, 12 mM $MgCl_2$ and 30 mM KCl during 20 min at room temperature. Some assays contained 50 nM of *Neisseria meningitidis* $tRNA^{Asp}$ transcript. Ten-microliter samples were analyzed by native PAGE (8%) in 89 mM Tris-Borate pH 8.3 at 4°C. Free and protein-bound [^{32}P] labeled tRNAs were revealed by scanning the image plates after 12 h exposure with a Fuji Bioimager and quantified using the volume rectangle tool of the Quantify One Software (BIO-RAD).

Activity assays

ATP–[^{32}P]PPi exchange was performed in 300 μl reaction mixtures containing 100 mM Na-HEPES pH 7.2, 5 mM $MgCl_2$, 2 mM ATP, 2 mM [^{32}P]PPi (1–2 cpm·pmol^{-1}), 1 mM L-Gln, 0.5 mg·ml^{-1} bovine serum albumin, 2 mg·ml^{-1} total *D. radiodurans* tRNA and appropriate amounts of FL- or Δ-GlnRSs. For K_M measurements, concentrations of $tRNA^{Gln}$ and Gln varied, respectively from 0.1 to 3 μM and from 0.7 to 10 mM for FL-GlnRS and from 0.5 to 10 μM and from 1 to 20 mM for Δ-GlnRS, the non-varied ligands being saturating. The [^{32}P]ATP formed at 37°C was determined in 50-μl aliquots (29).

For tRNA aminoacylation, 25 μl reaction mixtures contained 100 mM Na-HEPES pH 7.2, 2 mM ATP, 10 mM $MgCl_2$, 30 mM KCl, 0.5 mg·ml^{-1} bovine serum albumin, 50 μM L-[^{14}C]Gln (351 cpm·pmol^{-1}), 1–2 mg·ml^{-1} *D. radiodurans* unfractionated tRNA (Gln charging:0.8 nmol·mg^{-1}) or 1–2 μM $tRNA^{Gln(UUG)}$ or $tRNA^{Gln(CUG)}$ transcripts (Gln charging:25 nmol·mg^{-1}) and appropriate amounts of FL- or Δ-GlnRS for initial rate or plateau measurements. For Gln K_M determinations, reaction mixtures contained 10–100 μM L-[^{14}C]Gln and a saturating concentration of tRNA; for tRNA K_M determinations they contained 5 μM L-[^{3}H]Gln (560 cpm·pmol^{-1}) and 1.74–10.9 or 10–111 nM $tRNA^{Gln}$ in the presence of FL- and Δ-GlnRS, respectively or either 0.2–1 μM or 2–75 μM $tRNA^{Gln(UUG)}$ transcript. The amount of [^{3}H] or [^{14}C]glutaminyl-tRNA formed after incubations from 30 s to 30 min at 37°C was determined in 10-μl aliquots (29).

Crystallographic methods, structure analysis and modeling

Crystals of *Dr* GlnRS diffracting at 2.3 Å resolution were grown in microbatch in the presence of PEG 3350 (24). The structure was solved by molecular replacement (MR) using the structure of *Ec* GlnRS as a search model (30). The MR solution was refined with CNS (31) using a maximum likelihood target, a bulk solvent correction and a set of 7% of the reflections randomly selected for free R-factor testing. After rigid-body refinement, alternate simulated annealing and B-factor refinement rounds followed by a stepwise increase of resolution from 3 to 2.3 Å, the R- and free R-factors dropped from 50.9 and 51.1% to 25.6 and 29.8%, respectively. Several loops of the model were rebuilt manually in O (32). Water molecules developing sensible H-bonds with protein or other solvent atoms were finally added, leading to final R- and free R-factors of 20.0 and 24.2%, respectively. The final model includes 556 amino acids (A43-W632) and 160 water molecules. The N-terminal tail (M1-P42), the C-terminal extension (G633-A852) and two loops in the anticodon-binding domain (N537-Q564 and D614-A619) are not seen even in electron density maps computed at lower resolutions. Structure validation was performed with PROCHECK (33). The structure has been deposited with the Research Collaboratory for Structural Bioinformatics Protein Data Bank (PDB code: 2HZ7).

Structures of *Ec* GlnRS, either in the free state (PDB id: 1NYL) or in complex with ligands (tRNA, AMP, Gln; PDB id: 1O0B) were used for comparison with that of *Dr* GlnRS using LSQMAN (34). Superimposition was performed with a distance cutoff of 3.5 Å. Root-mean-square deviation (RMSD) values determined for the whole GlnRS-core or individual domains are based on equivalent main chain atom positions (N, Cα, C). This structural superimposition allowed annotation of the alignment.

A normal mode analysis of the structure of *Dr* GlnRS based on the elastic network model was performed using the ElNemo web service (34,35). Sets of normal mode perturbed models were generated for the first five low frequency modes. The model showing the lowest RMSD with *Ec* GlnRS complexed with the ligands obtained by combining mode 7 and 9 was used for tRNA docking. A series of models, intermediate between the latter and the X-ray structure, were used to predict a plausible conformational pathway between the free and tRNA-bound states. The regions of the enzyme that are not observed in the electron density map and, thus are absent in the current structure, were modeled using Modeller (36). The C-terminal domain was derived from alignment of the Yqey domains and the structure of the Yqey protein of *Bacillus subtilis* (PDB id: 1NG6).

RESULTS

Dr GlnRS is a structural hybrid between conventional GlnRS and AdT

The structural organization of *Dr* GlnRS was established by separate multiple sequence alignments. A first alignment of known bacterial GlnRSs shows that *Dr* GlnRS is highly similar to other bacterial GlnRSs, with the exception of a few insertions (17, 27 and 5 additional residues in the structured region 410–433 and in two loops 535–565 and 610–620, respectively) and the presence of a short N-terminal extension (M1–A43) and a long C-terminal appendix (G633–A862) (Figure 1A). This high degree of homology suggests that *Dr* GlnRS,

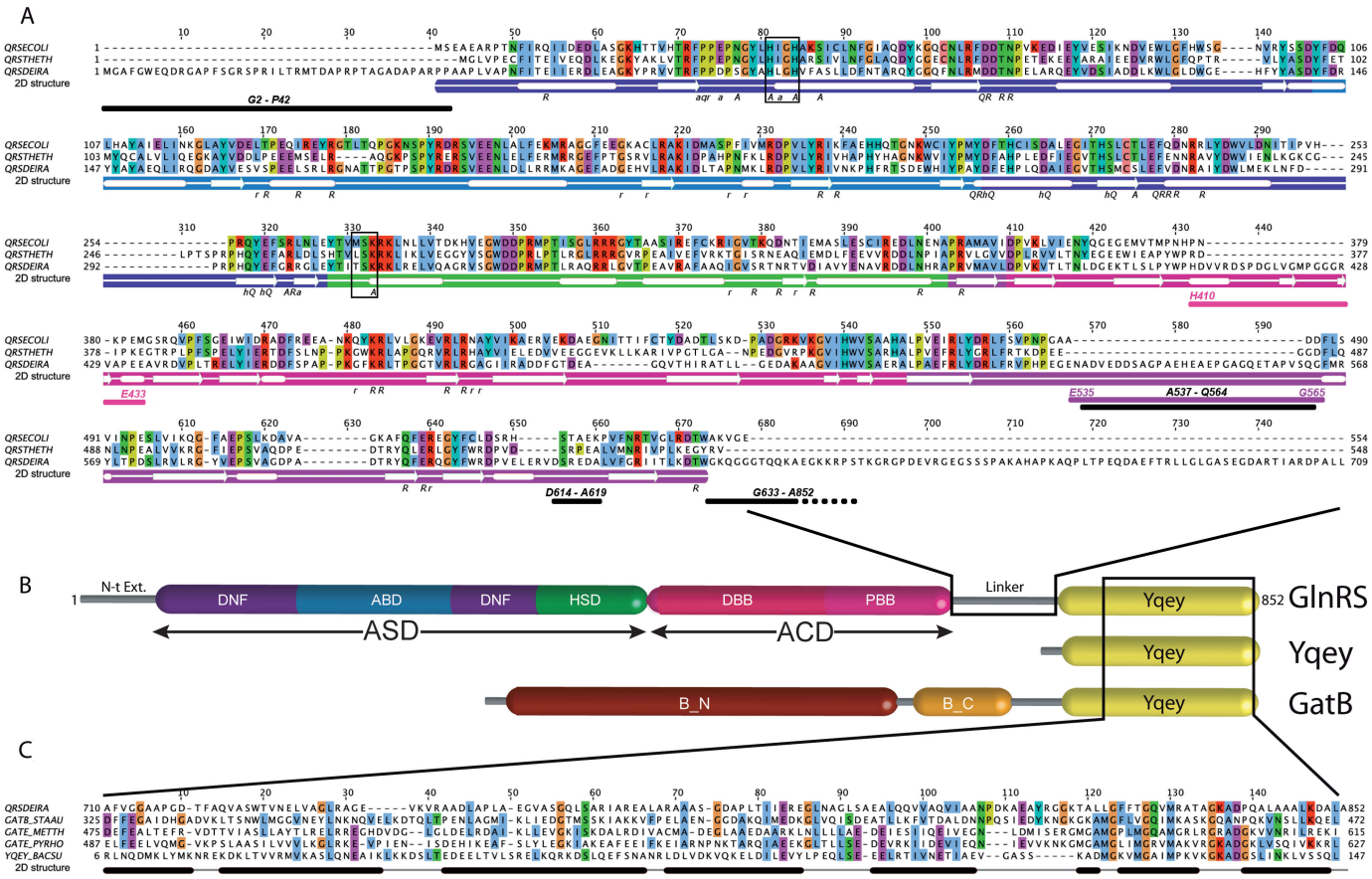

Figure 1. Comparative alignments of *Dr* GlnRS with bacterial GlnRSs and of related bacterial GatB with Yqey proteins and schematic description of the modular organization of these proteins. Panel (**A**): Structure-based sequence alignment of GlnRSs cores from *E. coli*, *T. thermophilus* and *D. radiodurans* (prepared with Jalview (37) and based on an alignment including 49 bacterial sequences). Residues are colored using the ClustalX scheme—orange: glycine (G); yellow: proline (P); blue: small and hydrophobic amino acids (A, V, L, I, M, F, W); green: hydroxyl and amide amino acids (S, T, N, Q); red: charged amino acids (D, E, R, K); cyan: histidine (H) and tyrosine (Y)—correspond to positions showing more than 40% identity. Secondary structure elements of *Dr* GlnRS determined using DSSP (38) are displayed below the sequences on a background using the following code to highlight the structural modules of the GlnRS core: from N- to C-terminus, dinucleotide fold (DNF) in dark blue, acceptor-stem binding domain (ABD) in light blue, helical subdomain (HSD) in green, distal and proximal beta-barrels (DBB and PBB) in magenta and violet, respectively. Residues interacting in *E. coli* binary and ternary complexes (1O0B, 1GTR) with ATP/AMP, Gln/5′O[*N*-(L-Gln)sulfamoyl] adenosine and tRNA are indicated by A (a), Q (q) or R (r), respectively (lower case letters are for main-chain interactions, upper case letters for side-chain contacts) and hQ stands for side-chain interactions with glutamine mediated by H_2O molecules. The regions of the enzyme that are not observed in the electron density map are underlined by black lines. The two long insertions of *Dr* GlnRS are highlighted and class I motives HL/IGH and T/MSK are boxed. Panel (**B**): Schematic organization of the three representative architectures of the Yqey family (PFAM 02637). For GlnRS, ASD and ACD stand for active side domain and anticodon domain, respectively, with structural modules abbreviated as indicated in (A); for GatB, (B_N) and (B_C) are the N- and C-terminal regions, respectively. Panel (**C**): Alignement of the C-terminus of *Dr* GlnRS and other members of the Yqey family (based on the PFAM description of this α-helical domain (PFAM 02637)). Residues displaying at least 40% identity are highlighted with color code as in (B). The secondary structure of *B. subtilis* Yqey (PDB id: 1NG6) is indicated.

like the *E. coli* enzyme (30), has a modular architecture (Figure 1B). Moreover, most residues contacting substrates in *Ec* GlnRS (20,30) are conserved in *Dr* GlnRS.

Next, the C-terminal appendix of *Dr* GlnRS was aligned with all known Yqey sequences, including that of *B. subtilis*, and with those of bacterial GatB and GatE proteins (Figure 1C). This alignment shows a moderate degree of sequence similarity, since out of the 215 amino acids constituting the extension of *Dr* GlnRS, only the 150 most distal align with other Yqey proteins, with highest similarity in the 30 last residues (Figure 1C).

The relatively weak sequence homology between the Yqey domain of *Dr* GlnRS and GatB subunits raises the question of their conformational homology. A first answer came from an immunological approach. Western blots (Figure 2A) show that *Dr* GlnRS is recognized by anti-AdT antibodies (lane 2) specific to the GatA and GatB subunits of *T. thermophilus* AdT (lane 1). These antibodies do not recognize *T. thermophilus* GlnRS (Figure 2A, lane 3) lacking Yqey (39), suggesting that anti-GatB antibodies recognize the Yqey domain of *Dr* GlnRS. The unambiguous proof of this assumption came from comparative experiments done with three GlnRS variants, namely a truncated form lacking the entire Yqey domain (Δ-GlnRS), a full length Yqey domain of 220 amino acids (FL-Yqey) and a deletion variant of the extension without the 61 residue-long linker (Δ-Yqey). Δ-GlnRS is no longer recognized by

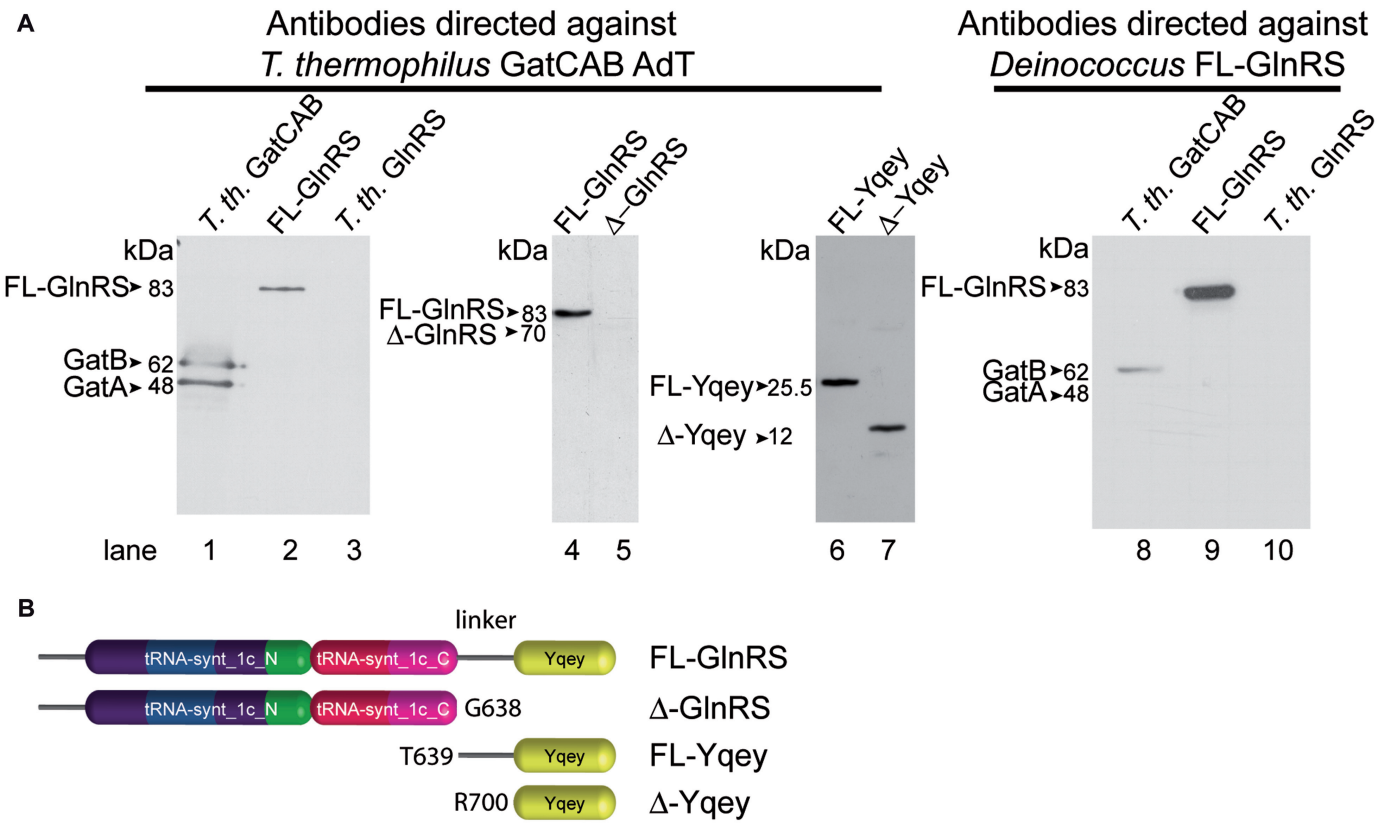

Figure 2. Analysis of the structural relationship between Yqey domains of *Dr* GlnRS and bacterial GatB by Western - blots. (**A**) Western-blot analyses using antibodies directed against *T. thermophilus* GatCAB AdT or *Dr* GlnRS. The proteins analyzed are indicated on the top of the lanes. (**B**) Schematic representation of the full length and deletion mutants of *Dr* GlnRS used in this analysis. The nature and the position of the last or the first amino acids of the different GlnRS variants are indicated on the basis of the amino acid numbering of FL-GlnRS; in panel (B) tRNA-synt_1c_N and tRNA-synt_1c_C indicate the N- and C-terminal regions of the class Ic GlnRS and Yqey, the Yqey domain.

the anti-GatB antibodies, while both FL-Yqey and Δ-Yqey are recognized (Figure 2A, lanes 5–7). Thus, the Yqey domain of *Dr* GlnRS is solely responsible for the cross-reaction with anti-GatB antibodies. Conversely, antibodies directed against *Dr* GlnRS, specifically recognize GatB from *T. thermophilus* AdT and not GatA (Figure 2A, lanes 8 and 9). Additionally, these antibodies are unable to recognize *T. thermophilus* GlnRS indicating the absence of common epitopes in the core of both enzymes (Figure 2A, lane 10). Altogether this demonstrates a structural resemblance between the Yqey domain of *Dr* GlnRS and the family of Yqey proteins. In other words, it confirms the chimerical nature of *Dr* GlnRS suspected from sequence analysis.

Crystallographic structure of *Dr* GlnRS

FL-GlnRS forms orthorhombic crystals that diffract X-rays beyond 2.3 Å resolution. The structure was solved by molecular replacement with the *E. coli* enzyme in complex with the ligands (PDB id: 1O0B) giving the best score (40). In total, 556 residues corresponding to the classical GlnRS-core in the N-terminal region of the protein were built and refined. Unexpectedly, about one-third of the protein is not observed in the crystal packing, despite the good quality of the diffraction data (Table 1) and the resulting electron density maps (Supplemental Figure 1). The missing parts are the N-terminal tail, two loops of the GlnRS-core and the C-terminal domain. A proteolytic degradation is excluded since the integrity of the protein in the crystals was confirmed by SDS-PAGE and mass spectrometry. This suggests that the missing parts of the protein are not trapped but remain mobile to a certain extent in the packing, an interpretation supported by additional physico-chemical investigations (to be published). At the present stage, analysis of crystal packing and solvent content (44% and Matthews coefficient 2.2 $Å^3$/Da) indicates that the $P2_12_12_1$ crystals can accommodate FL-GlnRS. This implies that the ordered part of the protein only represents 38% of the unit cell volume.

As could be anticipated from sequence conservation and straightforward molecular replacement, the GlnRS-core is similar to that of *E. coli* (Figure 3A). The structures can be superimposed with a RMSD of 1.9–2.3 Å (Supplemental Table 1 for RMSD analysis). Below, the *E. coli* nomenclature is used to describe the protein which can be divided as follows: an active site domain (ASD) composed of a Rossmann or dinucleotide fold (DNF) and the acceptor-stem binding domain (ABD), an intermediate helical subdomain (HSD) and the anticodon-binding domain (ACD) made of a proximal and a distal β-barrel (PBB, DBB).

Table 1. Summary of X-ray data collection and structure refinement statistics

Data collection	
X-ray source	ID14-1 (ESRF)
Space group	$P2_12_12_1$
Cell parameters a, b, c (Å)	74.1, 95.9, 115.7
Resolution range (Å)	2.3–30
No. of observations	209 589
No. of unique reflections	36 991
Completeness (%)	98.1 (92.9)[a]
R_{merge} (%)	6.2 (25.0)[a]
Average $I/\sigma(I)$	18.1 (5.5)[a]
Refinement	
R-factor (%)	20.0 (25.5)[a]
Free *R*-factor (%)	24.2 (29.1)[a]
No. of atoms	
Protein	4488
Water molecules	160
Average B-factors (Å^2)	
Overall	41.7
Protein	41.6
Water molecules	42.3
RMSD for bonds (Å), angles (°)	0.009, 1.5
Ramachandran plot (%)	
Most favored	90.2
Additional allowed	9.3
Generously allowed	0.4

[a]Last resolution shell: 2.30–2.36 Å.

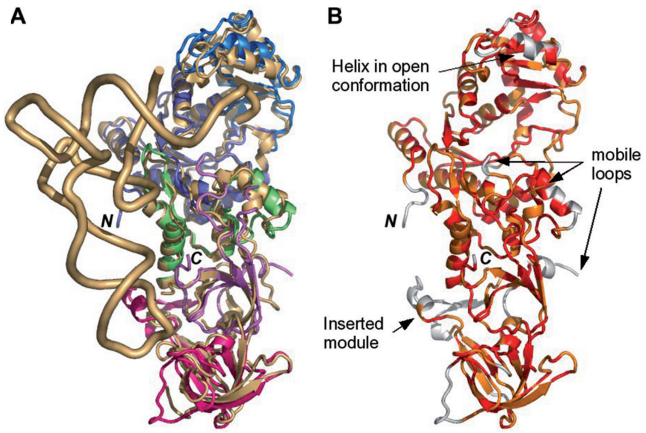

Figure 3. Comparison of *Ec* and *Dr* GlnRSs. (**A**) *Ec* GlnRS in complex with cognate tRNA, Gln and AMPCPP (40) (overall structure colored in gold) is superimposed to the visible core of *Dr* GlnRS (this study). Domains of the latter are depicted in distinct colors and their definition follows the nomenclature of the *E. coli* system (41). Color code from N- to C-terminus: dinucleotide fold in dark blue, acceptor-stem binding domain in light blue, helical subdomain in green, proximal and distal beta-barrels in violet and magenta, respectively. (**B**) This picture of *Dr* GlnRS highlights in orange and red all common positions that are superimposed with a distance lower than 3.5 Å. In contrast, white patches reveal the regions which are structurally different. Regions with strictly conserved amino acids are in red.

Figure 3B highlights the sequence and structure conservations between *Ec* and *Dr* GlnRS*s*. The ASDs of the two proteins are similar and present the HI/LGH and T/MSK signatures of class I synthetases. This part of both GlnRSs is deprived of any insertion–deletion sequence. The unique difference concerns position of a helix in the ABD which varies from more than 3.5 Å (depicted in white in Figure 3B). It adopts an open conformation in *Dr* GlnRS and closes upon tRNA binding in the ligand-complexed *Ec* GlnRS. Overall, low RMSD values (0.8–1.3 Å) are observed in the ASD, as well as in the HSD.

The major structural differences between *Ec* and *Dr* GlnRSs occur in their ACDs. The PBB of *Dr* GlnRS contains two insertions in surface loops that are not seen in the density. The first consists of 27 residues forming an extended loop (535–565) located at the bottom of the catalytic cleft; this element is replaced by a short turn in *Ec* GlnRS. The second concerns five additional residues in a loop (610–620) opposite to the anticodon-loop binding site. The PBB has been proposed as a module promoting communication between the catalytic center and the DBB where the anticodon of tRNA is bound. Accordingly, this part of the structure shows the highest RMSD deviations with the complexed *Ec* GlnRS. The DBB of *Dr* GlnRS also carries other idiosyncrasies, namely an additional element of 34 residues (410–433) that folds in a helix followed by two short β-strands sitting next to the minor groove of the anticodon stem of tRNA and a deletion of 8 residues found in a loop that would be close to nucleotides 34–36 of the tRNA anticodon. This loop (497–505) is well defined in *Dr* GlnRS whereas it has not been observed in the structure of *Ec* GlnRS either in free form or complexed with the substrates, probably due to a greater mobility related to its larger size. Overall, this domain appears to be more rigid than the PBB as revealed by RMSD values of 1.2–1.3 Å.

The amino acids of *Ec* GlnRS shown to participate in binding of the substrates are almost fully conserved in *Dr* GlnRS: all residues involved in recognition of Gln by direct or solvent mediated interactions are present, as well as most residues constituting the ATP pocket. Even more striking is the high level of conservation of the residues which in *Ec* GlnRS develop specific interactions with tRNA (Figure 1A).

Among the 40 residues of *Ec* GlnRS which contact tRNA (12 with main-chain atoms and 28 with lateral-chain atoms) 25 are strictly conserved and 9 present structural conservative changes (e.g. Ile/Leu, Glu/Gln) in *Dr* GlnRS. Interestingly, 4 residues of *Dr* GlnRS are unable to make the interactions described for the *E. coli* complex. Among the 10 residues of *Ec* GlnRS contacting ATP, 8 are conserved or substituted by equivalent residues and the 13 contacting Gln are conserved, except one substituted by a functionally equivalent residue (M of the MSK motif replaced by T) (Supplemental Table 2).

Effect of Yqey on the kinetic properties of GlnRS

Preliminary assays with total *D. radiodurans* tRNA showed same aminoacylation plateaus with Δ- and FL-GlnRSs, suggesting that Δ-GlnRS does not mischarge a non-cognate tRNA. The plateau obtained with FL-GlnRS does not increase after addition of Δ-GlnRS, showing that both enzymes charge the same tRNA. However, to obtain the same plateau, a significantly higher concentration of Δ-GlnRS than of FL-GlnRS

Table 2. Activities of full length and C-terminal truncated *D. radiodurans* GlnRS

	GlnRS activities					
	ATP–[^{32}P]PP$_i$ exchange			tRNA Aminoacylation		
Substrate	FL-GlnRS	Δ-GlnRS		FL-GlnRS	Δ-GlnRS	
	K_M (μM)		LK_M	K_M (μM)		LK_M
Gln	1000	2130	2.13	186	168	0.9
tRNA^{Gln} (n)	0.062	6.25	101	0.064	1.54	24
tRNA^{Gln} (t)	nd	nd		0.120	>27	>225
	k_{cat} (s^{-1})		Lk_{cat}	k_{cat} (s^{-1})		Lk_{cat}
tRNA^{Gln} (n)	44	26	1.7	5.73	1.25	4.6
tRNA^{Gln} (t)	Nd	nd	nd	0.15	nm	nm
	k_{cat}/K_M ($\mu M^{-1}\cdot s^{-1}$)		Lk_{cat}/K_M	k_{cat}/K_M ($\mu M^{-1}\cdot s^{-1}$)		Lk_{cat}/K_M
tRNA^{Gln} (n)	710	4.2	170	89.5	0.83	108
tRNA^{Gln} (t)	nd	nd	nd	1.25	4.5×10^{-6}	2.78×10^5

Each value is an average of at least two independent determinations. tRNA^{Gln} (n): native modified tRNA^{Gln} in total *D. radiodurans* tRNA; tRNA^{Gln} (t): tRNA$^{Gln(UUG)}$ transcript. Losses in affinity for the ligands (LK_M), in the catalytic rate (Lk_{cat}) and in catalytic efficiency (Lk_{cat}/K_M) between FL- and Δ-GlnRSs are expressed as K_M of Δ-GlnRS over K_M of FL-GlnRS, k_{cat} of FL-GlnRS over k_{cat} of Δ-GlnRS and k_{cat}/K_M of FL-GlnRS over k_{cat}/K_M of Δ-GlnRS, respectively. nd: not determined; nm: non measurable. Standard deviation of data is ∼20%.

is required, indicating that deletion of Yqey alters the catalytic properties of the enzyme.

Comparative experiments deciphered the effects of Yqey on the catalytic properties of *Dr* GlnRS. First Δ-GlnRS, like FL-GlnRS and other GlnRSs, requires cognate tRNA for Gln activation. Further, the kinetic constants of Gln activation and tRNA aminoacylation (Table 2) show that both FL- and Δ-GlnRSs exhibit similar K_M's for Gln in ATP–PPi exchange as well as in tRNA charging, suggesting that Yqey is not involved in binding of the amino-acid substrate. This activation is specific since the two enzyme forms do not catalyze Glu-dependent ATP–[^{32}P]PPi exchange under the conditions where Gln promotes the exchange and despite the ability of *Ec* GlnRS to bind Glu (40). On the other hand, FL- and Δ-GlnRSs catalyze amino-acid activation and tRNA aminoacylation, with similar rate since deletion of the Yqey domain only slightly decreases k_{cat}'s of ATP–PPi exchange and tRNA charging (Table 2). This suggests that Yqey does not contain essential residues for catalysis or active conformation of the enzyme. The domain, however, increases the affinity of the enzyme for cognate tRNA^{Gln}, as revealed by the significant K_M decrease of FL-GlnRS for this substrate, especially pronounced for ATP–PPi exchange. Taken together, the Yqey flexible module increases the catalytic efficiency of GlnRS for both tRNA^{Gln}-dependent Gln activation and tRNA^{Gln} charging and is involved in binding of tRNA^{Gln} to GlnRS.

Next, the capacity of *Dr* GlnRS to make a functional distinction between its two tRNA^{Gln} isoacceptors, tRNA$^{Gln(UUG)}$ and tRNA$^{Gln(CUG)}$, and the possible role of Yqey in this distinction, were investigated. Thus charging of the two transcripts by FL- and Δ-GlnRSs was tested. In contrast to *Ec* GlnRS that charges transcript and modified tRNA^{Gln} with similar efficiencies (42), *Dr* GlnRS aminoacylates the tRNA$^{Gln(UUG)}$ transcript significantly less efficiently than modified tRNA^{Gln} and the two transcripts with distinct rates, the tRNA$^{Gln(UUG)}$ transcript being charged one order of magnitude faster than the tRNA$^{Gln(CUG)}$ transcript (not shown). Further, Δ-GlnRS charges the tRNA$^{Gln(UUG)}$ transcript one order of magnitude slower than FL-GlnRS and is unable to charge the tRNA$^{Gln(CUG)}$ transcript to a detectable level (not shown). This indicates that *Dr* GlnRS can charge the two isoacceptors, although with distinct efficiencies and that Yqey does not support preferential aminoacylation of one of them. Interestingly, the two tRNAs display 73% identity. Sequence analysis shows that among the elements determining glutaminylation of *E. coli* tRNA^{Gln} (43–45), 10 are conserved in *D. radiodurans* tRNA$^{Gln(UUG)}$ (G73, G2–C71, G3–C70, G10, U34, U35 and G36, U38) and 8 in tRNA$^{Gln(CUG)}$ (G73, G2–C71, G3–C70, G10, U35, G36, U1–A72). Among the positions involved in *E. coli* glutaminylation, both tRNAs differ by positions 1–73, 34 and 38 (respectively A1–U73, U34, U38 and U1–A73, C34, C38 in tRNA$^{Gln(UUG)}$ and tRNA$^{Gln\ (CUG)}$).

Interestingly, the above data suggest a role of post-transcriptional modifications in tRNA aminoacylation (Table 2). FL-GlnRS aminoacylates modified tRNA$^{Gln(UUG)}$ ∼80-fold more efficiently than the transcript as a result of a strong k_{cat} increase and a faint K_M decrease. The poor affinity of Δ-GlnRS for the tRNA$^{Gln(UUG)}$ transcript did not allow determination of the individual kinetic constants for the unmodified molecule. However, under first-order kinetic conditions with respect to tRNA, the k_{cat}/K_M ratio could be measured directly. It indicates that Δ-GlnRS aminoacylates the transcript ∼5 order of magnitude less efficiently than FL-GlnRS. Since the absence of Yqey decreases charging efficiency of the transcript much more than that of native tRNA^{Gln} (∼23 000-fold), participation of the post-transcriptional modifications in the Yqey-dependent formation of the competent GlnRS·tRNA^{Gln} complex is not a side effect. It is specific to *D. radiodurans* tRNA^{Gln} since modified *E. coli* tRNA^{Gln} is a poor substrate for *Dr* GlnRS (not shown). The nature of the peculiar modifications in *D. radiodurans* tRNA^{Gln} awaits

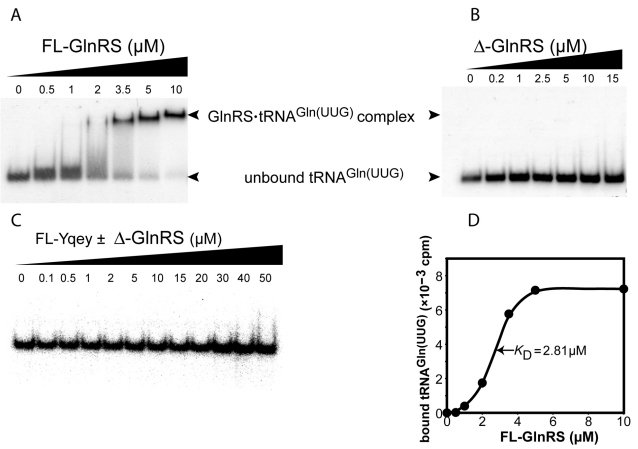

Figure 4. Analysis of the binding of $tRNA^{Gln(UUG)}$ to FL-GlnRS (**A**), Δ-GlnRS (**B**) and FL-Yqey domain with or without Δ-GlnRS (**C**) by gel retardation and determination of the K_D of the FL-GlnRS·$tRNA^{Gln(UUG)}$ complex (**D**). Gel shifts were performed with 5×10^5 cpm of [^{32}P]-labeled $tRNA^{Gln(UUG)}$ transcript and 0–10 μM of FL-GlnRS or 0–15 μM Δ-GlnRS or 0–50 μM FL-Yqey or 0–50 μM Δ-GlnRS and FL-Yqey.

to be characterized. Interestingly, it has been shown that in *E. coli* the post-transcriptionally modified nucleotides of $tRNA^{Gln}$ are not involved in glutaminylation (44).

Effect of Yqey on tRNA binding on GlnRS

Binding of $tRNA^{Gln}$ on FL- and Δ-GlnRSs, and on FL-Yqey, was analyzed by gel retardation. Figure 4A shows, as expected, a shift of the [^{32}P]-labeled $tRNA^{Gln(UUG)}$ transcript when migrating with FL-GlnRS. An apparent dissociation constant (K_D) of 2.8 μM could be calculated for the complex (Figure 4D). Binding is specific as incubation with a 100-fold excess of $tRNA^{Asn}$ transcript did not displace $tRNA^{Gln(UUG)}$ from the enzyme. In contrast, Δ-GlnRS is incapable to interact with $tRNA^{Gln(UUG)}$ transcript throughout the range of protein concentrations assayed, as no mobility shift of labeled tRNA occurs (Figure 4B). Further, no shift was observed when increasing Δ-GlnRS concentration up to 50 μM. This confirms that removal of Yqey suppresses the tRNA-binding capacity of *Dr* GlnRS.

Given this crucial contribution of Yqey in *Dr* GlnRS for binding $tRNA^{Gln}$, the capacity of FL-Yqey (Figure 4C) and Δ-Yqey domains to bind the $tRNA^{Gln(UUG)}$ transcript was checked. Both Yqey variants are unable to shift the cognate tRNA transcript, even at very high protein concentrations. Thus, isolated Yqey is not a tRNA binder *per se*. Furthermore this domain is unable to restore in *trans* (i.e. by addition of increasing amounts of FL- or Δ-Yqey domains), a $tRNA^{Gln}$-binding capability to Δ-GlnRS (Figure 4C).

The GlnRS·$tRNA^{Gln}$ complex of *D. radiodurans*

To gain insight into the implication of each region of the *Dr* GlnRS in substrate binding, a model of the FL-GlnRS in complex with $tRNA^{Gln}$ was built (Figure 5). The *Dr* GlnRS was docked onto the *Ec* GlnRS·$tRNA^{Gln}$ complex and the missing C-terminal domain was modeled

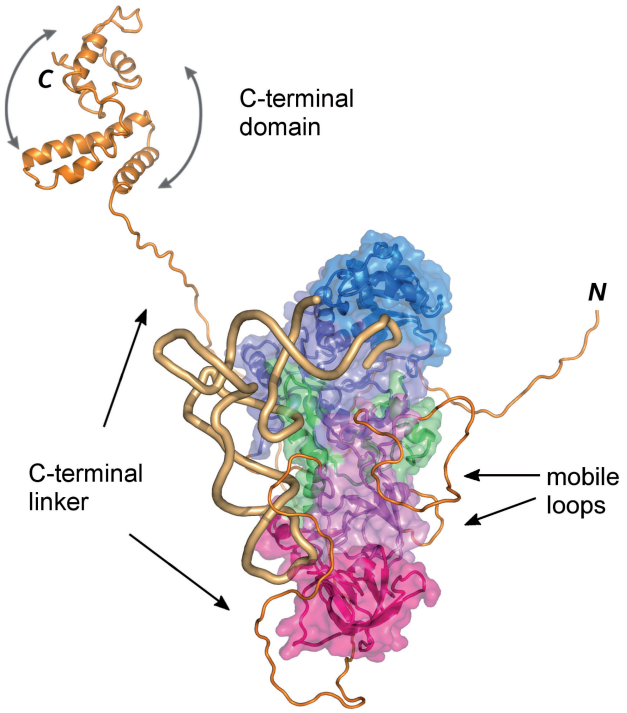

Figure 5. Model of *D. radiodurans* GlnRS·$tRNA^{Gln}$ complex. Residues of the GlnRS core described in the X-ray structure are depicted with the same color code as in Figure 3. Amino acids that are not observed in the experimental electron density map have been modeled and are shown in orange. The *Dr* GlnRS structure was perturbed using a normal mode analysis in order to fit the conformation with that of the complexed *Ec* GlnRS and to dock the tRNA as observed in the *Ec* complex. N and C refer to the N- and C-terminal ends of the protein. The model illustrates the unusual length and flexibility of the N-terminal tail, the large PBB loop close to the active site and the C-terminal domain. The Yqey-like appendix is located at the end of a 60–80 residues long linker and can potentially interact with any part of the tRNA or of the GlnRS because of its flexibility highlighted by the arrows.

using the structure of *B. subtilis* Yqey protein. The Yqey extension could be easily constructed in the architecture found in the crystal structure of *B. subtilis* Yqey (PDB id: 1NG6). Its location in Figure 5 is revealing since it can move on the flexible hinge linker, as implied by its disordered location in the *Dr* GlnRS crystals that otherwise show good perfection. The model indicates that the Yqey domain can easily interact with any region of the GlnRS core or of the tRNA. In addition, normal mode analysis suggests a conformational pathway similar to that described for the *Ec* GlnRS·$tRNA^{Gln}$ complex: a closure of the enzyme upon tRNA binding and a simultaneous rotation of the anticodon-binding domain with respect to the catalytic core (not shown).

DISCUSSION

Unprecedented properties of the Yqey domain from *Dr* GlnRS

As the EMAPII-like domain present in aaRSs and involved in tRNA binding, Yqey exists either in a free form or as an aaRS-appendix. However, contrasting with free EMAPII formed through a proteolytic cleavage of the p43 protein (46) and to which a cellular function

could be attributed (47–49), Yqey is synthesized in free form in many bacteria like *B. subtilis* (21), and its function, remains elusive. In yeast mitochondria, where it constitutes the Pet-112 protein, it can be complemented in a Pet-112 deficient strain, by *B. subtilis* GadB, a paralog of Yqey (50). Notably, Yqey is found only exceptionally in aaRSs and has been identified in only 3 GlnRSs, namely those of *Deinococcus geothermalis* and *Salinibacter ruber* (Blast NCBI) in addition to that of *D. radiodurans* (this study). It constitutes the unique additional domain found in prokaryotic GlnRSs.

The present study establishes that the Yqey domain of *Dr* GlnRS is an actor in tRNA aminoacylation and suggests that it contributes to tRNA binding. More precisely, kinetic data unambiguously show that Yqey is a tRNA affinity enhancer for *Dr* GlnRS. Yqey must be covalently attached to the GlnRS core to fullfil its role, since it is unable to act in *trans* when added in free form to the truncated enzyme. Its connection through a long polypeptide linker to GlnRS constitutes another peculiarity distinguishing Yqey from other aaRS-appended modules. This feature confers unprecedented properties to *Dr* GlnRS.

Formation of the catalytically competent GlnRS·tRNA^{Gln} complex triggered by Yqey is tuned by the modified nucleotides of tRNA, as supported by kinetic data. Although the details of this tuning remain to be deciphered, it appears that the modifications contribute more to the formation of a competent complex than to the primary binding of tRNA. The way whereby Yqey enhances affinity of *Dr* GlnRS for native post-transcriptionally modified tRNA^{Gln} is intriguing since the core enzyme conserves most of the residues of *Ec* GlnRS involved in tRNA recognition, and thus is expected to be fully competent to charge efficiently tRNA^{Gln}. Because appended Yqey increases k_{cat} of tRNA charging and decreases K_M, it may act by two ways, either in favoring formation of the competent complex by distorting and reorienting the partners to a productive state or in increasing affinity of GlnRS for tRNA^{Gln} by enhancing the rate of complex formation and decreasing that of its dissociation.

Finally, from the viewpoint of prokaryote genomes, *Yqey* genes are often located in an operon (Supplemental Table 3). The gene of ribosomal S21 protein is mostly found associated with that of Yqey, but other genes can also be found, although less frequently. The grouping of Yqey and S21 genes in an operon is independent of the presence or absence of AdT and when present, independent of its activity, either Glu- or Asp-AdT. Protein S21 is peculiar to eubacteria and S21-deficient 30S ribosomes are unable to bind mRNA and to initiate protein synthesis in *E. coli* (51). Assuming that Yqey-containing operons encode proteins of related functions, Yqey may be a cofactor involved in protein synthesis.

Expected features and idiosyncrasies in atypical *Dr* GlnRS: functional implications

Sequence comparison of *Dr* GlnRS with other bacterial GlnRSs predicts architectural similarities of these enzymes. The prediction was verified by crystallography, with the core of *Dr* GlnRS similar to that of *Ec* GlnRS. Given this fact, and because most of the residues involved in substrate binding are conserved, one could *a priori* expect that *Dr* GlnRS would be fully functional in the absence of its Yqey appended domain. This is not the case and the serendipitous findings of a Yqey participation in tRNA binding and of the poor binding capacity of Δ-GlnRS, were surprises. Moreover, the Yqey domain by itself is a very weak tRNA binder. These surprising observations can be rationalized assuming the Yqey extension is involved in the formation of the productive GlnRS·tRNA^{Gln} complex.

In a structural perspective, and at first glance, the insertions observed in the core enzyme cannot easily account for the observations. However, although crystallography does not yet answer unambiguously how the extension participates in the aminoacylation function of *Dr* GlnRS, it does not exclude a direct contact of the Yqey domain with tRNA. This domain contains helical subdomains that may allow such contacts with tRNA helices, as found in the yeast AspRS extension (52), but their content of basic residues is poor, except for the most proximal helix to the GlnRS core (Figure 1). The linker making the connection with this core is long enough to allow Yqey to contact any region of the tRNA, even its acceptor or anticodon ends (Figure 5). If so, the extension would clamp the tRNA on the GlnRS core in position optimal for activity. Reminiscent to what occurs in the *Ec* GlnRS·tRNA^{Gln} complex, where base-pair U1–A72 opens prior entry of the tRNA^{Gln}-acceptor end in the catalytic site (30), and in AdT-systems where this pair is a recognition determinant for amidation of tRNA-bound Glu or Asp into Gln or Asn (23,53), Yqey in *Dr* GlnRS may trigger the formation of the competent complex by contacting the U1–A72 pair of tRNA^{Gln}. Additional structural data are awaited to test this hypothesis and to decipher the puzzling tRNA recognition by *Dr* GlnRS. However, the presence of Yqey in free form regardless whether GlnRS is present or absent in the organism such as in *B. subtilis* deprived of GlnRS and which uses the indirect pathway for Gln-tRNA^{Gln} formation (4), suggests that this domain may exert additional functions not directly related to Gln-tRNA^{Gln} formation, like stabilization of the aa-tRNA, regulation of its synthesis, or coupling of its synthesis with other metabolic pathways. Alternatively, it cannot be excluded that even in free form Yqey participates in cellular functions involving protein–nucleic acids interactions such as binding to an aaRS·tRNA complex to increase efficiency and/or specificity of tRNA aminoacylation. In this case, the protein's properties would resemble Ybak (54,55) which binds Cys-tRNA^{Pro} complexed with ProRS and promotes hydrolysis of the mischarged tRNA. However, it does so by acting exclusively in *trans*, in contrast to the role of Yqey in *Dr* GlnRS, which can be performed only when it is present in *cis*.

Considerations about evolution of tRNA glutaminylation and asparaginylation led to the proposal that the transamidation pathway constitutes the primitive route to Gln-tRNA^{Gln} and Asn-tRNA^{Asn} formation (9,10).

These routes preceded the emergence of the modern GlnRS and AsnRS, able to synthesize their corresponding aa-tRNAs by charging preformed Gln and Asn onto their cognate tRNAs (9,10). Thus, by amidating Glu and Asp charged on $tRNA^{Gln}$ and $tRNA^{Asn}$, AdT was probably the first enzyme able to form Asn and Gln for protein synthesis purposes. Sequence comparisons and phylogenetic trees revealed that GlnRS evolved from a duplicated gene of GluRS in eukaryotes, and was transferred in various eubacterial species by lateral gene transfer (5). In *D. radiodurans*, Gln-$tRNA^{Gln}$ is formed by the modern GlnRS whereas Asn-$tRNA^{Asn}$ is formed by the indirect pathway involving AdT (13). In this organism recruitment, by GlnRS, of a domain belonging to the AdT, a partner of the ancient pathway of Gln-$tRNA^{Gln}$ and Asn-$tRNA^{Asn}$ synthesis is surprising, and reveals an unexpected interrelation between the ancient and the modern pathways of amide aa-tRNA formation. Since the Yqey domain is only exceptionally appended to bacterial GlnRS, fusion of both occurred late in evolution and was probably related to acquisition of peculiar properties of GlnRS. Investigations are underway to identify the precise functions of the free and GlnRS-bound Yqey.

ACKNOWLEDGEMENTS

This work was supported by the Université Louis Pasteur (Strasbourg), Centre National de la Recherche Scientifique (CNRS), and grants from Association pour la Recherche sur le Cancer (ARC) and ACI Biologie Cellulaire, Moléculaire et Structurale. The authors acknowledge the team of ID14 beamlines at ESRF for assistance during data collection. M.D. benefitted from FEBS and CNRS grants and C.S. was the recipient of a Marie Curie European Reintegration Grant (MERG-CT-2004-004898). Funding to pay the Open Access publication charge was provided by the CNRS.

Conflict of interest statement. None declared.

REFERENCES

1. Schimmel,P. and Söll,D. (1979) Aminoacyl-tRNA synthetases: general features and recognition of transfer RNAs. *Annu. Rev. Biochem.*, **48**, 601–648.
2. Ibba,M., Becker,H.D., Stathopoulos,C., Tumbula,D.L. and Söll,D. (2000) The adaptor hypothesis revisited. *Trends Biochem. Sci.*, **25**, 311–316.
3. Tumbula,D.L., Becker,H.D., Chang,W-Z. and Söll,D. (2000) Domain-specific recruitment of amide amino acids for protein synthesis. *Nature*, **407**, 106–110.
4. Curnow,A.W., Hong,K.-W., Yuan,R., Kim,S., Martins,O., Winkler,W., Henkin,T.M., Söll,D. *et al.* (1997) Glu-$tRNA^{Gln}$ amidotransferase: a novel heterotrimeric enzyme required for correct decoding of glutamine codons during translation. *Proc. Natl. Acad. Sci. U.S.A.*, **94**, 11819–11826.
5. Lamour,V., Quevillon,S., Diriong,S., N'Guyen,V.C., Lipinski,M. and Mirande,M. (1994) Evolution of the Glx-tRNA synthetase family: the glutaminyl enzyme as a case of horizontal gene transfer. *Proc. Natl. Acad. Sci. U.S.A.*, **91**, 8670–8674.
6. Salazar,J.-C., Zúñiga,R., Raczniak,G., Becker,H. D., Söll,D. and Orellana,O. (2001) A dual-specific Glu-$tRNA^{Gln}$ and Asp-$tRNA^{Asn}$ amidotransferase is involved in decoding glutamine and asparagine codons in *Acidithiobacillus ferrooxidans*. *FEBS Lett.*, **500**, 129–131.
7. Raczniak,G., Becker,H.D., Min,B. and Söll,D. (2001) A single amidotransferase forms asparaginyl-tRNA and glutaminyl-tRNA in *Chlamydia trachomatis*. *J. Biol. Chem.*, **276**, 45862–45867.
8. Lapointe,J., Duplain,L. and Proulx,M. (1986) A single glutamyl-tRNA synthetase aminoacylates $tRNA^{Glu}$ and $tRNA^{Gln}$ in *Bacillus subtilis* and efficiently misacylates *Escherichia coli* $tRNA^{Gln}_1$ in vitro. *J. Bacteriol.*, **165**, 88–93.
9. Kern,D., Roy,H. and Becker,H.D. (2005). Chapter 20, Asparaginyl-tRNA synthetases: pathways and evolutionary history of tRNA asparaginylation. In: Ibba,M., Francklyn,C. and Cusack,S. (eds), *Aminoacyl-tRNA synthetases*. Landes Bioscience, Georgetown, US.
10. Feng,L.F., Tumbula-Hansen,D., Min,B., Namgoong,S., Salazar,J., Orellana,O. and Söll,D. (2005). Chapter 32, Transfer RNA-dependent amidotransferases key enzymes for Asn-tRNA and Gln-tRNA synthesis in nature. In: Ibba,M., Francklyn,C. and Cusack,S. (eds), *Aminoacyl-tRNA synthetases*. Landes Bioscience, Georgetown, US.
11. Schmitt,E., Panvert,M., Blanquet,S. and Mechulam,Y. (2005) Structural basis for tRNA-dependent amidotransferase function. *Structure*, **13**, 1421–1433.
12. White,O., Eisen,J.A., Heidelberg,J.F., Hickey,E.K., Peterson,J.D., Dodson,R.J., Haft,D.H., Gwinn,M.L., Nelson,W.C. *et al.* (1999) Genome sequence of the radioresistant bacterium *Deinococcus radiodurans* R1. *Science*, **286**, 1571–1577.
13. Curnow,A.W., Tumbula,D.L., Pelaschier,J.T., Min,B. and Söll,D. (1998) Glutamyl-$tRNA^{Gln}$ amidotransferase in *Deinococcus radiodurans* may be confined to asparagine biosynthesis. *Proc. Natl. Acad. Sci. U.S.A.*, **95**, 12838–12843.
14. Jasin,M., Regan,L. and Schimmel,P. (1983) Modular arrangement of functional domains along the sequence of an aminoacyl tRNA synthetase. *Nature*, **306**, 441–447.
15. Delarue,M. and Moras,D. (1993) The aminoacyl-tRNA synthetase family: modules at work. *Bioessays*, **10**, 675–687.
16. Moras,D. (1992) Structural and functional relationship betweeen aminoacyl-tRNA synthetases. *Trends Biochem. Sci.*, **17**, 159–164.
17. Cusack,S. (1997) Aminoacyl-tRNA synthetases. *Curr. Opin. Struct. Biol.*, **6**, 881–889.
18. Schimmel,P. and Ribas De Pouplana,L. (2000) Footprints of aminoacyl-tRNA synthetases are everywhere. *Trends Biochem. Sci.*, **25**, 207–209.
19. Freist,W., Gauss,D.H., Ibba,M. and Söll,D. (1997) Glutaminyl-tRNA synthetase. *Biol. Chem.*, **378**, 1103–1117.
20. Sherlin,L.D. and Perona,J.J. (2003) tRNA-dependent active site assembly in a class I aminoacyl-tRNA synthetase. *Structure*, **11**, 591–603.
21. http://www.sanger.ac.uk//cgi-bin/Pfam/getacc?PF02637
22. Nakamura,A., Yao,M., Chimnaronk,S., Sakai,N. and Tanaka,I. (2006) Ammonia channel couples glutaminase with transamidase reactions in GatCAB. *Science*, **312**, 1954–1958.
23. Oshikane,H., Sheppard,K., Fukai,S., Nakamura,Y., Ishitani,R., Numata,T., Sherrer,R.L., Feng,L., Schmitt,E. *et al.* (2006) Structural basis of RNA-dependent recruitment of glutamine to the genetic code. *Science*, **312**, 1950–1954.
24. Deniziak,M.A., Sauter,C., Becker,H.D., Giegé,R. and Kern,D. (2004) Crystallization and preliminary X-ray characterization of the atypical glutaminyl-tRNA synthetase from *Deinococcus radiodurans*. *Acta Crystallogr. D. Biol. Crystallogr.*, **60**, 2361–2363.
25. Chomczynski,P. and Sacchi,N. (1987) Single-step method of RNA isolation by acid guanidinium thiocyanate-phenol-chloroform extraction. *Anal. Biochem.*, **162**, 156–159.
26. Becker,H.D., Giegé,R. and Kern,D. (1996) Identity of prokaryotic and eukaryotic $tRNA^{Asp}$ for aminoacylation by aspartyl-tRNA synthetase from *Thermus thermophilus*. *Biochemistry*, **35**, 7447–7458.
27. Fechter,P., Rudinger,J., Giegé,R. and Theobald-Dietrich,A. (1998) Ribozyme processed tRNA transcripts with unfriendly internal promoter for T7 RNA polymerase: production and activity. *FEBS Lett.*, **436**, 99–103.
28. Prevost,G., Eriani,G., Kern,D., Dirheimer,G. and Gangloff,J. (1989) Study of the arrangement of the functional domains along the yeast cytoplasmic aspartyl-tRNA synthetase. *Eur. J. Biochem.*, **180**, 351–358.

29. Kern,D. and Lapointe,J. (1979) The twenty aminoacyl-tRNA synthetases from *Escherichia coli*. General separation procedure and comparison of the influence of pH and divalent cations on their catalytic activities. *Biochimie*., **61**, 1257–1272.
30. Rould,M.A., Perona,J.J., Söll,D. and Steitz,T.A. (1989) Structure of *E. coli* glutaminyl-tRNA synthetase complexed with $tRNA^{Gln}$ and ATP at 2.8 Å resolution. *Science*, **246**, 1135–1142.
31. Brünger,A.T., Adams,P.D., Clore,G.M., DeLano,W.L., Gros,P., Grosse-Kunstleve,R.W., Jiang,J.S., Kusezewski,J., Nilges,M. *et al.* (1998) Crystallography and NMR system: a new software suite for macromolecular structure determination. *Acta Crystallogr. D. Biol. Crystallogr.*, **54**, 905–921.
32. Kleywegt,G.J., Zou,J.Y., Kjeldgaard,M. and Jones,T.A. (2001). Around O. In: Rossmann,M.G. and Arnold,E. (eds), *International Tables for crystallography*. Volume F. *Crystallography of Biological Macromolecules*. Kluwer Academic Publishers, Dortrecht, The Netherlands, pp. 353–356 and 366–367.
33. Laskowsky,R.A., Rullmann,J.A., MacArthur,M.W., Kaptein,R. and Thornton,J.M. (1996) AQUA and PROCHECK-NMR: programs for checking the quality of protein structures solved by NMR. *J. Biomol. NMR*, **8**, 477–486.
34. http://www.igs.cnrs-mrs.fr/elnemo/
35. Suhre,K. and Sanejouand,Y.H. (2004) EINemo: a normal mode web server for protein movement analysis and the generation of templates for molecular remplacement. *Nucleic Acids Res.*, **32** (Web Server issue) W610–W614.
36. Sali,A., Potterton,L., Yuan,F., van Vlijmen,H. and Karplus,M. (1995) Evaluation of comparative protein modeling by MODELLER. *Proteins*, **23**, 318–326.
37. Clamp,M, Cuff,J., Searle,S.M. and Barton,G.J. (2004) The Jalview Java Alignment editor. *Bioinformatics Appl. Note*, **20**, 426–427.
38. Kabsch,W. and Sander,C. (1983) Dictionary of protein secondary structure: pattern recognition of hydrogen-bonded and geometrical features. *Biopolymers*, **12**, 2577–2637.
39. Henne,A., Bruggemann,H., Raasch,C., Wiezer,A., Hartsch,T., Liesegang,H., Johann,A., Lienard,T., Gohl,O. *et al.* (2004) The genome sequence of the extreme thermophile *Thermus thermophilus*. *Nat. Biotechnol.*, **22**, 547–553.
40. Bullock,T.L., Uter,N., Nissan,T.A. and Perona,J.J. (2003) Amino acid discrimination by a class I aminoacyl-tRNA synthetase specified by negative determinants. *J. Mol. Biol.*, **328**, 395–408.
41. Perona,J. (2005). Glutaminyl-tRNA synthetases. In: Ibba,M., Francklyn,C. and Cusack,S. (eds), *Aminoacyl-tRNA synthetases* Landes Bioscience, Georgetown, US., pp. 73–88.
42. Ibba,M., Hong,K.-W., Sherman,J.M., Sever,S. and Söll,D. (1996) Interactions between tRNA identity nucleotides and their recognition sites in glutaminyl-tRNA synthetase determine the cognate amino acid affinity of the enzyme. *Proc. Natl. Acad. Sci. U.S.A.*, **93**, 6953–6958.
43. Hayase,Y., Jahn,M., Rogers,M.J., Sylvers,L.A., Koizumi,M., Inoue,H., Ohtsuka,E. and Söll,D. (1992) Recognition of bases in *E. coli* $tRNA^{Gln}$ by glutaminyl-tRNA synthetase: a complete identity set. *EMBO J.*, **11**, 4159–4165.
44. Jahn,M., Rogers,M.J. and Söll,D. (1991) Anticodon and acceptor stem nucleotides in $tRNA^{Gln}$ are major recognition elements for *E. coli* glutaminyl-tRNA synthetase. *Nature*, **352**, 258–260.
45. Ibba,M., Hong,K. W. and Söll,D. (1996) Glutaminyl-tRNA synthetase: from genetics to molecular recognition. *Genes Cells*, **1**, 421–427.
46. Quevillon,S., Agou,F., Robinson,J.C. and Mirande,M. (1997) The p43 component of the mammalian multi-synthetase complex is likely to be the precursor of the endothelial monocyte-activating polypeptide II cytokine. *J. Biol. Chem.*, **272**, 32573–32579.
47. Wagasuki,K. and Schimmel,P. (1999) Two distinct cytokines released from a human aminoacyl-tRNA synthetase. *Science*, **284**, 147–151.
48. Kao,J., Houck,K., Fan,Y., Haehnel,L., Libutti,S. K., Kayton,M.L., Grikscheit,T., Chabot,J., Nowygrod,R.B. *et al.* (1994) Characterization of a novel tumor-derived cytokine endothelial monocyte activating polypeptide II. *J. Biol. Chem.*, **269**, 25106–25119.
49. Knies,U.E., Behrensdorf,H.A., Mitchell,C.A., Deutsch,U., Risau,W., Drexler,H.C. and Clauss,M. (1998) Regulation of endothelial monocyte-activating polypeptide II release by apoptosis. *Proc. Natl. Acad. Sci. U.S.A.*, **95**, 12322–12327.
50. Kim,S.L., Stange-Thomann,N., Martins,O., Hong,K.W., Söll,D. and Fox,T.D. (1997) A nuclear genetic lesion affecting *Saccharomyces cerevisiae* mitochondrial translation is complemented by a homologous gene. *J. Bacteriol.*, **179**, 5625–5627.
51. Van Duin,J. and Wijnands,R. (1981) The function of ribosomal protein S21 in protein synthesis. *Eur. J. Biochem.*, **118**, 615–619.
52. Frugier,M., Moulinier,L. and Giegé,R. (2000) A domain in the N-terminal extension of class IIb eukaryotic aminoacyl-tRNA synthetases important for tRNA binding. *EMBO J.*, **19**, 2371–2380.
53. Bailly,M., Giannouli,S., Blaise,M., Stathopoulos,C., Kern,D. and Becker,H.D. (2006) A single base-pair mediates bacterial tRNA-dependent biosynthesis of asparagine. *Nucleic Acids Res.*, **34**, 6083–6094.
54. Ruan,B. and Söll,D. (2005) The bacterial Ybak protein is a Cys-$tRNA^{Pro}$ and Cys-$tRNA^{Cys}$ deacylase. *J. Biol. Chem.*, **280**, 25887–25891.
55. An,S. and Musier-Forsyth, (2005) Cys-$tRNA^{Pro}$ editing by *Haemophilus influenzae* Ybak via a novel Synthetase.Ybak.tRNA ternary complex. *J. Biol. Chem.*, **280**, 34465–34472.